Effect of process parameters on mechanical and tribological performance of pulsed-DC sputtered TiC/a-C

Shaha, K.P.; Pei, Y.T.; Martinez-Martinez, D.; Sanchez-Lopez, J.C.; Hosson, J.Th.M. De

Published in:
Surface & Coatings Technology

DOI:
10.1016/j.surfcoat.2010.10.020

Surface & Coatings Technology 205 (2010) 2633–2642

Contents lists available at ScienceDirect

Surface & Coatings Technology

journal homepage: www.elsevier.com/locate/surfcoat

Effect of process parameters on mechanical and tribological performance of pulsed-DC sputtered TiC/a-C:H nanocomposite films

K.P. Shaha [a], Y.T. Pei [a], D. Martinez-Martinez [a], J.C. Sanchez-Lopez [b], J.Th.M. De Hosson [a,*]

[a] Department of Applied Physics, Materials innovation institute M2i, University of Groningen, Nijenborgh 4, 9747 AG Groningen, The Netherlands
[b] Instituto de Ciencia de Materiales de Sevilla (CSIC-Universidad de Sevilla), Avda. Americo Vespucio 49, 41092-Sevilla, Spain

ARTICLE INFO

Article history:
Received 27 August 2010
Accepted in revised form 6 October 2010
Available online 11 October 2010

Keywords:
DLC
Nanocomposite
TiC/a-C:H
Pulsed-DC
Tribological performance
Raman spectroscopy

ABSTRACT

Mechanical, structural, chemical bonding (sp^3/sp^2), and tribological properties of films deposited by pulsed-DC sputtering of Ti targets in Ar/C_2H_2 plasma were studied as a function of the substrate bias voltage, Ti-target current, C_2H_2 flow rate and pulse frequency by nanoindentation, Raman spectroscopy and ball-on-disc tribometry. The new findings in this study comprise: dense, column-free, smooth, and ultra-low friction TiC/a-C:H films are obtained at a lower substrate bias voltage by pulsed-DC sputtering at 200 and 350 kHz frequency. The change in chemical and phase composition influences the tribological performance where the TiC/a-C:H films perform better than the pure a-C:H films. In the case of TiC/a-C:H nanocomposite films, a higher sp^2 content and the presence of TiC nanocrystallites at the sliding surface promote formation of a transfer layer and yield lower friction. In the case of a-C:H films, a higher sp^3 content and higher stress promote formation of hard wear debris during sliding, which cause abrasive wear of the ball counterpart and yield higher friction.

1. Introduction

Nanocomposite thin films have recently attracted increasing interest due to the possibility of the synthesis of materials with unique properties, e.g. super-hardness [1,2], combined hardness and low friction [3], or "chameleonic" or surface adaptative [4]. Diamond like carbon (DLC) films are of significant interest because of their unique combination of chemical–physical properties, high wear resistance and low friction [5]. Nanocomposite coatings based on dispersion of TiC nanocrystalline phases in solid lubricant phases like amorphous carbon (a-C) or amorphous hydrocarbon (a-C:H) have been shown to enhance the hardness and toughness while maintaining the low coefficient of friction [6–10]. Such films show great potential for exploitation as a protective and lubricant layer to enhance the wear resistance of many tribological applications in ambient air or in vacuum. Various deposition techniques such as chemical vapor deposition [11], DC reactive magnetron sputtering [6,12], cathodic arc deposition [13,14], and pulsed laser deposition [7] have been employed for the synthesis of TiC/a-C or TiC/a-C:H films. Over the last decade, pulsed-DC (p-DC) magnetron sputtering has proven to be a versatile technique for deposition of advanced thin films. It was originally developed for the reactive deposition of insulating films to suppress arc events at the target and to stabilize the process. In addition, it has been observed that pulsing magnetrons increases ion energies and flux, plasma density and electron temperatures in the plasma, which often results in improved film microstructure and properties [15–18]. The Ar^+ ion and energy fluxes delivered to the growing film increase with increasing pulse frequency [15]. At a higher pulse frequency (350 kHz) a much extended Ar^+ ion energy distribution with a maximum ion energy beyond 200 eV was observed, which is much higher compared to that observed for DC sputtering (~20 eV) [15]. Hence, the effect of process parameters such as the substrate bias voltage or flow rate of reactive gas on the plasma properties could be different in magnitude to that occurring during DC sputtering. Moreover, in the case of reactive sputtering, the presence of the reactive gas can influence the plasma properties and hence the ion energy distribution at the substrate, which further may influence the properties of the films.

Thus, in this paper, the effect of process parameters viz., the substrate bias voltage, Ti-target current, C_2H_2 flow rate and pulse frequency, on the mechanical, structural (sp^3/sp^2) and tribological properties of films deposited by pulsed-DC magnetron sputtering of Ti targets in Ar/C_2H_2 plasma was studied in detail. The deposition conditions are correlated to the structural and mechanical properties of these films. Dense, tough and ultra-low friction TiC/a-C:H nanocomposite films were obtained under optimized conditions.

2. Experimental

TiC/a-C:H nanocomposite films were deposited on Si (100) wafers by close field unbalanced magnetron reactive sputtering with a TEER UDP400/4 system, which was configured of four magnetrons coupled to

* Corresponding author.
E-mail address: j.t.m.de.hosson@rug.nl (J.T.M. De Hosson).

0257-8972/$ – see front matter © 2010 Elsevier B.V. All rights reserved.
doi:10.1016/j.surfcoat.2010.10.020

three Ti targets and one Cr target and using Ar and acetylene (C_2H_2) gas sources. The size of all the targets was 200×100 mm². The magnetrons coupled to each of the two Ti targets mounted opposite to each other were powered by a Pinnacle Plus 5/5 kW double channel p-DC power supply (Advanced Energy) and the other two magnetrons coupled to Cr and Ti targets were powered by a Pinnacle 6/6 kW double channel DC power supply. The latter targets were used only during the deposition of a CrTi interlayer. All the power units for sputtering were operated in a current-control mode. The voltage applied to Ti targets reached up to 470 V. The substrates, located at 80 mm distant from the targets, were biased by a Pinnacle Plus 5 kW single channel p-DC power supply (Advanced Energy) at 250 kHz pulse frequency (50% duty cycle). The base pressure of the chamber before deposition was $3–4\times10^{-6}$ mbar. The substrates were first ultrasonically cleaned in acetone followed by Ar plasma etching for 15 min at p-DC −400 V bias voltage at 250 kHz and 87.5% duty cycle. A CrTi interlayer, having a thickness of approximately 150 nm, was deposited to improve the interfacial adhesion. Finally, two Ti targets were sputtered in a p-DC reactive mode in an Ar/C_2H_2 atmosphere to deposit the films. The substrate holder was rotated by 3 rpm. No external heating was applied to the substrates. The maximum temperature was measured at 120 °C during deposition of these films. To study the microstructure and deposition rate as a function of pulse frequency, the films were deposited at 0 (DC), 200 and 350 kHz pulse frequency (70% duty cycle). In order to investigate the effect of various process parameters on the mechanical and tribological properties of 200 kHz p-DC sputtered films, the negative substrate bias voltage, Ti-target current and the acetylene flow rate were varied in the range from 40 to 150 V, 0.6 to 1 A and 8 to 12 sccm, respectively. The flow rate of Ar gas was kept constant at 12 sccm for all the depositions. Furthermore, the properties of optimized (in terms of microstructure and composition) 200 kHz and 350 kHz p-DC sputtered TiC/a-C:H films were compared.

Electron probe microanalysis (EPMA) with a Cameca SX-50 spectrometer was used to determine the chemical composition of the films. The microstructure of these films was investigated by using a high resolution scanning electron microscope (SEM) (Philips FEG-XL30s) and an atomic force microscope (AFM) (Digital Instruments NanoScope IIIa) was used to characterize the surface morphology. Grazing incidence X-ray diffraction (XRD) spectra were acquired with a Bruker D8 diffractometer operating with a Cu Kα radiation source placed at 1.5° incident angle to the film surface. The average particle size in the different films was calculated from the full width at half maximum (FWHM) of the TiC (111) and (200) peaks using the Scherrer equation. A MTS Nanoindenter XP® was employed to measure the hardness (H) and modulus (E) of the films with a Berkovich indenter. The maximum indentation depth for measuring H and E was fixed at one tenth of the film thickness. Raman spectra by using a LabRAM Horiba Jobin Yvon spectrometer equipped with a CCD detector and a He–Ne laser (532 nm) at 5 mW for a wavelength range of 100–2000 cm^{-1} were acquired to investigate the chemical bonding of these films. The spectra were analyzed by the Breit–Wigner–Fano (BWF) line for the G peak and a Lorentzian fitting for the D peak as explained by Ferrari and J. Robertson in [19] with a linear background subtraction. The residual stress in selected films was measured by monitoring the curvature change of Φ50 mm Si-wafers before and after deposition. The tribological properties of these films were investigated using a CSM tribometer with a ball-on-disk configuration, against Φ6 mm 100Cr6 steel ball at a wear track radius of 9 mm at 10 cm/s sliding speed and 5 N normal load in humid air with a relative humidity of 50% at room temperature (~23 °C). The wear scar on the ball counterparts after the test was characterized by an optical microscope. A confocal microscope was used to capture 3D images on a wear track to measure wear volume of the films.

3. Results and discussion

The results are presented as follows. Firstly, the microstructural and surface morphological evolution of the nanocomposite films deposited by p-DC sputtering at different pulse frequencies is presented with particular emphasis on inhibiting the column formation. Then, the effect of the substrate bias voltage, phase and chemical composition on the mechanical and tribological properties of the a-C:H and TiC/a-C:H is discussed in detail. The synthesis conditions and properties of the films are summarized in Table 1. Finally, the effect of pulse frequency applied to the Ti target on the mechanical and tribological properties of the optimized TiC/a-C:H films (in terms of microstructure and composition) is evaluated and compared.

3.1. Microstructural evolution

Fig. 1 shows the cross sectional SEM micrographs of TiC/a-C:H nanocomposite films deposited for 120 min by DC and pulsed-DC sputtering at 200 and 350 kHz pulse frequency by keeping the current applied to Ti targets and C_2H_2 flow rate and substrate bias voltage fixed at 1 A and 8 sccm and 40 V, respectively. The film deposited by DC sputtering, as seen in Fig. 1a, exhibits strong columnar features. However, switching from DC to pulsed-DC sputtering at 200 and 350 kHz pulse frequency the microstructure evolves from columnar to column-free as seen in Fig. 1b and c, respectively. Since the column boundaries are a potential source of failure since they facilitate the crack initiation and propagation, a column-free microstructure is necessary for improved toughness under loading and contact sliding [20]. The dense, column-free films deposited by p-DC sputtering films are expected to be tougher than compared to the DC sputtered films.

The surface morphologies of these films are shown in Fig. 2. In the case of DC sputtering, as seen in Fig. 2a, the surface shows cauliflower morphology with peaks surrounded by a network of valleys and the peak-to-valley distance was large. However, in the case of p-DC sputtering, the peak-to-valley distance considerably decreases and the surface exhibits small ripples at 200 kHz (Fig. 2b) and nanosized bumps at 350 kHz (Fig. 2c). Consequently, a drastic decrease in surface rms roughness from about 8 nm for DC sputtered films to ~1.8 and 0.2 nm in the case of 200 and 350 kHz p-DC sputtered films, respectively, is observed. It must be noted that these films were deposited at 40 V. Thus, ultra-smooth films can be obtained by 350 kHz p-DC sputtering at a low substrate bias voltage. The Ar^+ ions energy and flux delivered to the growing film increases with increasing pulse frequency [15] and the enhanced surface diffusion driven growth [21] ascertains a smooth growth front and hence a column-free microstructure as explained in [22]. The microstructural and surface morphological evolutions of these films deposited by p-DC reactive sputtering as a function of pulse frequency are similar to those observed for films deposited by p-DC non-reactive sputtering [15].

It is important to note that the deposition rate of the p-DC sputtered films was lower than that observed for DC sputtering and depends on the pulse frequency. As compared to DC sputtering, approximately, 15 and 40% reduction in the deposition rate (see Fig. 1) was observed for p-DC sputtered TiC/a-C:H nanocomposite films at 200 and 350 kHz, respectively. The reduction in the deposition rate is due to a combination of several factors. The average power dissipated at the target decreases with increasing pulse frequency and at the start of each pulse there is a dead time during which negligible sputtering occurs and the proportion of this dead time increases with increasing pulse frequency and so the deposition rate is lower at a higher frequency [15,23]. The rate of voltage change at the target during the initial stages of the pulse-on period and the maximum negative voltage attained during the pulse-on period is significantly lower at higher frequencies [23]. Since sputtering rate is proportional to power and sputtering yield is proportional to target voltage, both these factors tend to lower the deposition rate at a higher frequency. The Ar^+ ion and energy flux to the substrate increases with the pulse frequency [15]. The higher ion to atom ratio at higher pulse

Table 1
Synthesis conditions (substrate bias voltage, Ti-Target current — I_{Ti}, C_2H_2 flow rate, and pulse frequency — f), chemical composition, surface rms roughness — R, Raman analysis (I(D)/I(G) ratio, position of G peak), mechanical properties (hardness — H, Young's modulus — E^*, and H/E^* ratio), residual stress — σ and tribological properties (coefficient of friction CoF and wear rate — Wr) of p-DC sputtered films.

	Bias (−V)	I_{Ti} (A)	C_2H_2 (sccm)	f (kHz)	Composition (at.%)			R (nm)	I(D)/I(G)	G-peak position	H (GPa)	E^* (GPa)	H/E^*	σ (− MPa)	CoF	Wr ($\times 10^{-7}$ mm^3/N m)
					Ti	C	O									
	40	1.0	8	200	17.31	79.80	1.37	1.85	0.91	1563.4	14.1	128.6	0.11	–	0.08	1.92
*	80				17.64	79.03	1.32	0.36	0.90	1562.6	15.8	142.6	0.11	–	0.09	1.60
	100				–	–	–	0.31	–	–	16.1	143.8	0.11	–	0.10	2.43
	150				17.82	78.98	1.21	0.23	0.74	1558.8	16.4	144.3	0.11	–	0.11	3.0
	80	0.6	8	200	0.28	96.16	0.69	–	–	–	24.5	178.1	0.14	–	0.15	–
**		0.75			12.47	84.09	1.07	0.61	0.73	1558.2	16.1	136.3	0.12	2158	0.05	0.66
*		1.0			17.64	79.03	1.32	0.36	0.90	1562.6	15.8	142.6	0.11	–	0.09	1.60
**	80	0.75	8	200	12.47	84.09	1.07	0.61	0.73	1558.2	16.1	136.3	0.12	2158	0.05	0.66
			10		0	96.31	0.20	0.69	0.25	1536.6	22.9	165.2	0.13	2418	0.10	1.14
			12		0	97.06	0.34	3.15	0.23	1534.8	23.8	168.1	0.14	2566	0.14	1.26
**	80	0.75	8	200	12.47	84.09	1.07	0.61	0.73	1558.2	16.1	136.3	0.12	2158	0.05	0.66
				350	12.19	84.30	1.08	0.52	0.49	1552.0	17.2	139.7	0.12	2808	0.07	0.82

Films marked with * and ** are repeated for clarity.

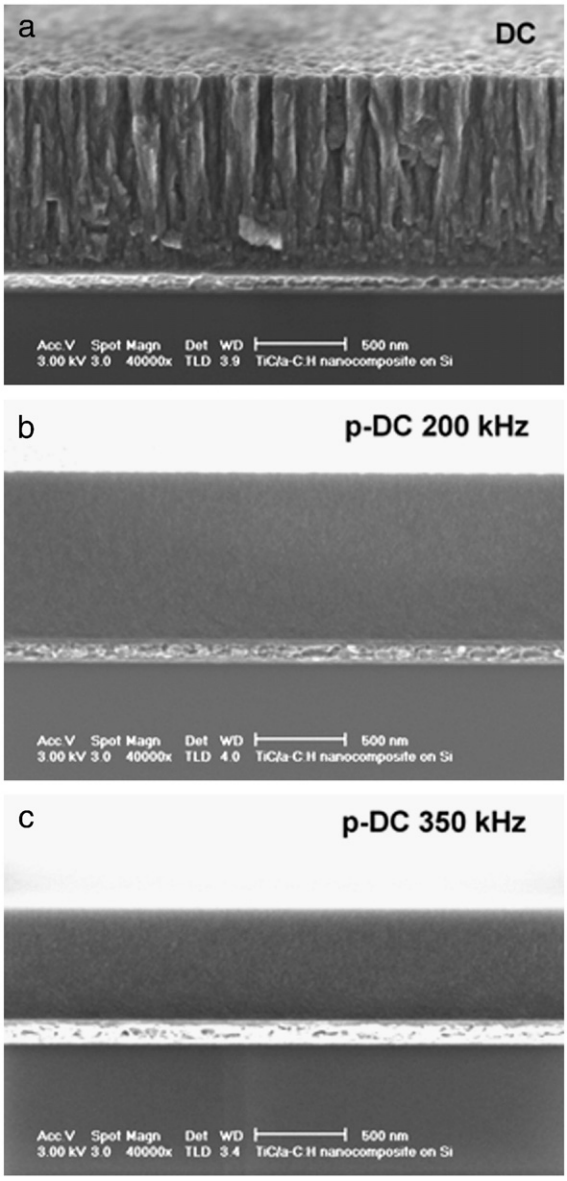

Fig. 1. Cross sectional SEM of TiC/a-C:H nanocomposite films deposited by (a) DC sputtering; and p-DC sputtering at (b) 200 kHz and (c) 350 kHz pulse frequency. (See text for detailed deposition conditions.)

frequencies would reduce the deposition rate by enhanced re-sputtering from the film. Since the reduction in deposition rate at 200 kHz was low, this was an optimal choice for further studying the influence of process parameters on the mechanical and tribological properties of these films.

3.2. Effect of the substrate bias voltage

In this section, the effect of the negative substrate bias voltage in the range from 40 to 150 V on the tribological, mechanical and structural properties of 200 kHz p-DC sputtered TiC/a-C:H nanocomposite films is discussed. The Ti-target current and C_2H_2 flow rate was kept constant at 1 A and 8 sccm, respectively. All these films exhibit glassy microstructure (not shown) and hence any possible effects of the columnar features on the properties of the films, particularly on friction and wear, were excluded. The Ti-content in these films was ~17.5 at.% and was not affected by changing the substrate bias voltage (See Table 1). The grazing incidence XRD analysis (not shown) confirmed formation of TiC nanocrystallites in these films. The average size of the TiC nanocrystallites for the films deposited at 40 and 150 V was 2.2 and 2.3 nm, respectively which indicates that the size of TiC nanocrystallites was not affected by the change in the substrate bias voltage. Fig. 3a demonstrates the tribotest results of the four films deposited at different bias voltages. All the films show a quick drop in the coefficient of friction (CoF) during the initial stages of sliding, which was mainly attributed to the quick formation of a transfer layer on the steel ball which facilitates easy sliding at the interface between the transfer layer and the TiC/a-C:H film. A transfer layer was observed on the steel balls after sliding against all these films (for e.g. as shown in Fig. 7c against the film deposited at 80 V). The transfer layer is believed to be formed by a friction-assisted phase transformation of the surface layer of the DLC [24], and is composed of mainly amorphous graphite-like carbon [25]. The friction graphs of the films deposited at lower bias voltages (40 and 80 V) are steady whereas jumps in CoF values are observed for the films deposited at higher bias voltages (100 and 150 V). Fig. 3b shows the CoF and hardness dependence of TiC/a-C:H nanocomposite films as a function of the substrate bias voltage. A moderate increase in CoF from 0.08 at 40 V to 0.11 at 150 V is observed. The hardness also shows a moderate increase from 14 GPa at 40 V to 16.5 GPa at 150 V. The wear rates of the films as a function of the substrate bias voltage are shown in Fig. 3c. Although the difference in the values is small, it can be seen that the wear rate is higher for films deposited at a higher substrate bias voltage. Despite the increase in hardness, the wear resistance of the films at higher bias values is reduced. Considerable wear debris were observed in and around the wear track after the tribotest on the films deposited at higher bias voltages (100 and 150 V). This also

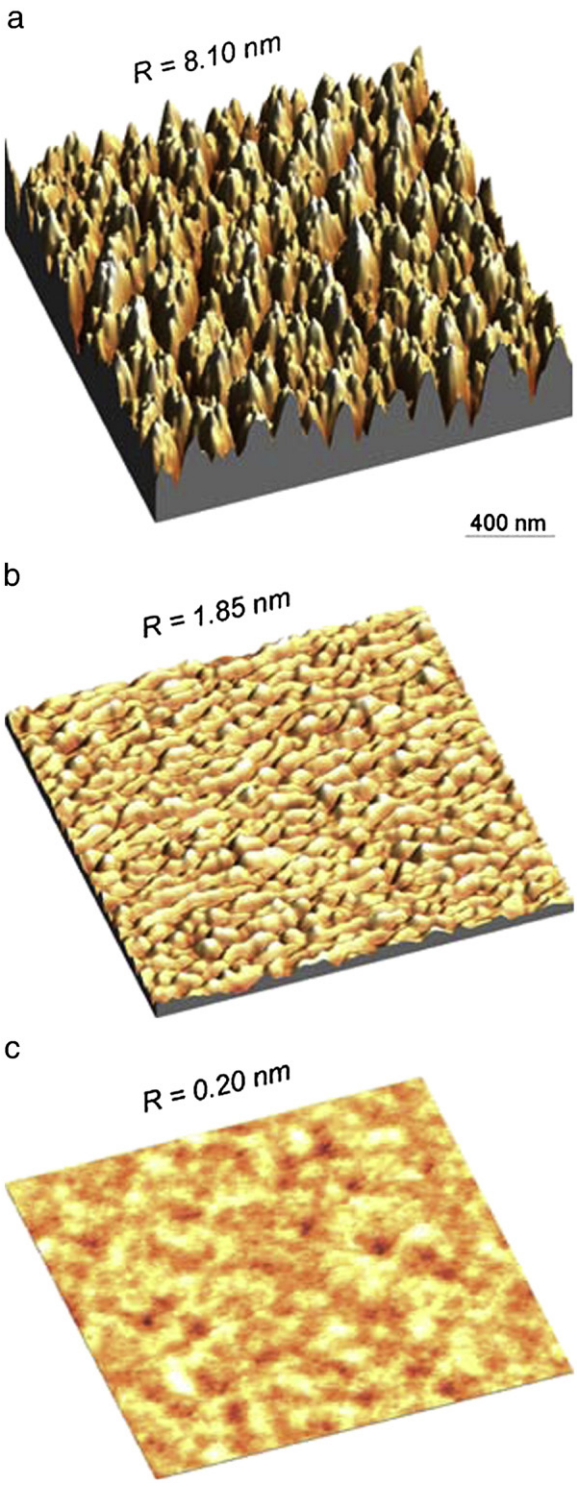

Fig. 2. AFM topography images of TiC/a-C:H nanocomposite films deposited by (a) DC sputtering; and p-DC sputtering at (b) 200 kHz and (c) 350 kHz pulse frequency. The corresponding RMS roughness (R) is indicated. (See text for detailed deposition conditions.)

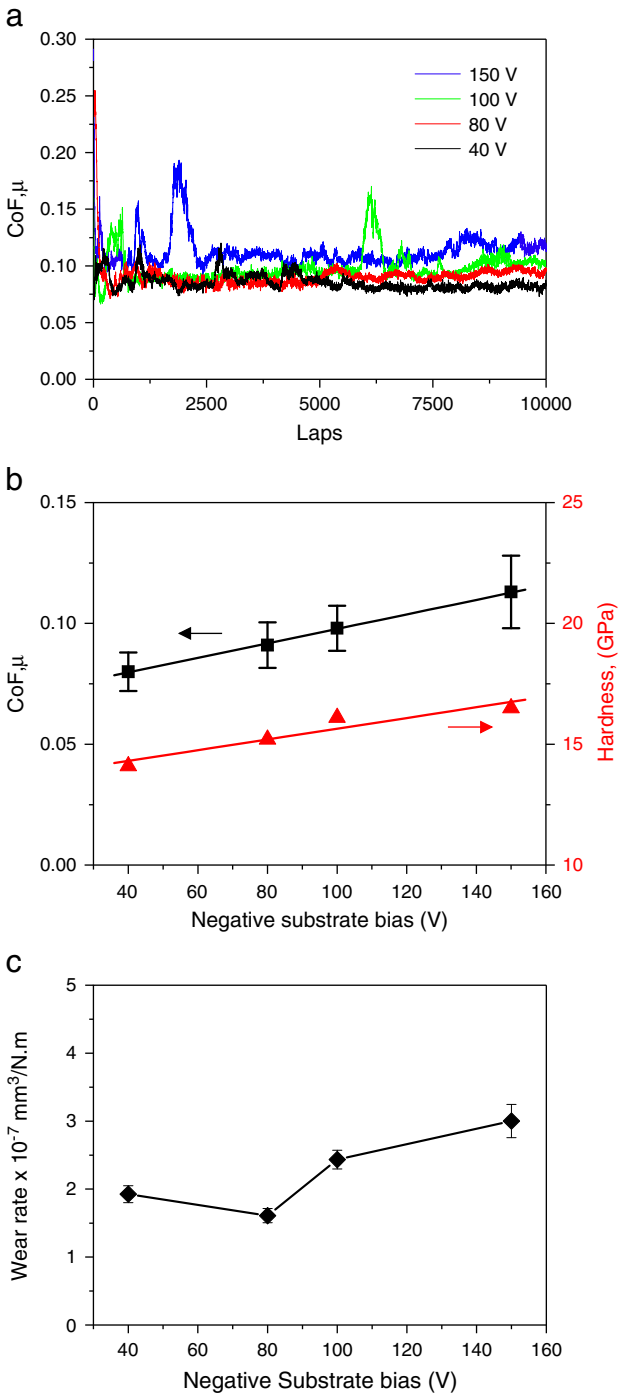

Fig. 3. (a) Friction characteristics of 200 kHz p-DC sputtered TiC/a-C:H films deposited at various negative substrate bias voltage, as indicated, sliding against steel ball at 5 N normal load, sliding velocity 10 cm/s and relative humidity of 50% at 23 °C; (b) CoF (■) and hardness (▲) and (c) wear rate of these films as a function of the negative substrate bias voltage.

reflects in the higher wear rates, in Fig. 3c, observed for these films. Since the presence of wear debris retards the transfer layer formation [26], it can be expected that the harder wear debris formed during the sliding against the films deposited at higher bias voltages hinder the formation of the transfer layer by means of three body abrasion. This also explains the fluctuations in CoF, as seen in Fig. 3a, observed for these films.

Raman analysis was carried out to understand the effect of the substrate bias voltage on the chemical structure (sp^3/sp^2) of these films. Fig. 4a and b shows the Raman spectra for the films deposited at 80 and 150 V substrate bias voltages. The Raman spectra show two distinct peaks; the so-called D peak at ~1350 cm^{-1} and the G peak at ~1580 cm^{-1}, which correspond to the so-called "disordered" and "graphitic" structures respectively. Ferrari and Robertson [19] showed the possibility of acquiring information of the hybridization states of C–C bonding from the analyses of the I(D)/I(G) ratio and the position of the G peak. Provided that the I(D)/I(G) ratio is in the range from 0.2

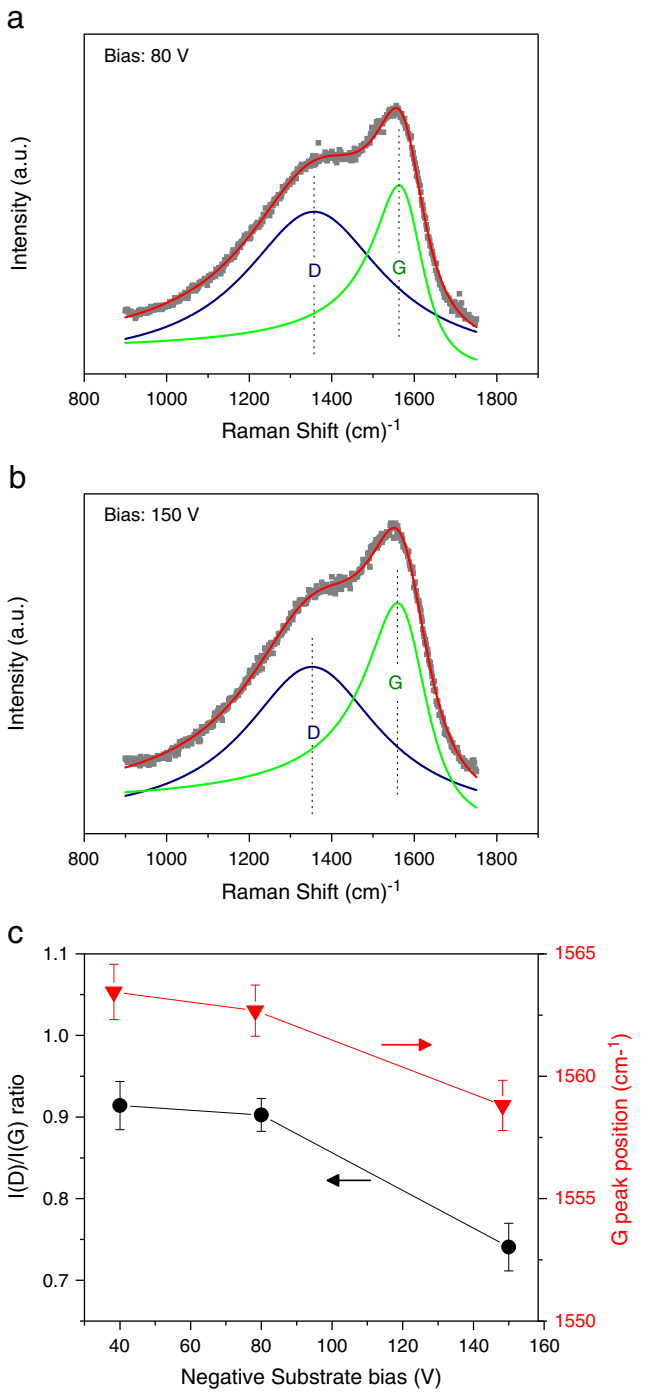

Fig. 4. BWF-Lorentzian fitted Raman spectra for TiC/a-C:H nanocomposite films deposited by 200 kHz p-DC sputtering at a negative substrate bias voltage of (a) 80 V and (b) 150 V; and (c) I(D)/I(G) ratio (●) and G peak position (▼) as a function of the negative substrate bias voltage for these films.

to 2 and the G peak position ranges from 1510 to 1600, a decrease in the I(D)/I(G) ratio and a shift of G peak to lower values indicate a progressive disordering of the sp^2-bonded rings and increase of sp^3 sites in the range from 0 to approximately 20% [19]. Fig. 4c shows the variation of the I(D)/I(G) ratio and G peak position as a function of the bias voltage. There was very little difference between the Raman spectra acquired from films deposited at 40 and 80 V. However, the I(D)/I(G) ratio decreases and the G peak shifts to a lower wavenumber for the film deposited at 150 V, indicating an increase in the sp^3 content in the film. The higher sp^3 content leads to an increase in the hardness at a higher substrate bias voltage similar to that observed by Martinez-Martinez et al. [27] in the case of pure amorphous carbon films. Also, it is relatively difficult to form a graphite-like transfer layer due to a relatively lower sp^2 content in the film and hence yields higher CoF. The increased ion energy delivered to the film at a higher substrate bias voltage may increase the compressive stress in the films [28,29] which facilitates the wear debris formation during sliding, as discussed later. Although the hydrogen content in the films was not measured, it may decrease with increasing substrate bias voltage [30], and thus contribute to higher CoF. Moreover, a direct correlation between high friction and high roughness is not observed since a relatively rougher film deposited at 40 V exhibits lower CoF. The influence of the substrate bias voltage on the surface roughness of these films is shown in Fig. 5. The surface rms roughness rapidly decreased from ~1.85 nm at 40 V to about 0.36 nm at 80 V and further reduced to about 0.23 nm at 150 V. A substrate bias voltage of 80 V was considered as optimum which yields a smooth surface and also avoids the higher stress in the film which otherwise deteriorates the tribological performance as that observed for films deposited at higher (100 and 150 V) substrate bias voltages.

3.3. Effect of phase and chemical composition

The composition of these films was varied by changing the Ti-target current and the acetylene flow rate, independently, but keeping the substrate bias voltage and pulse frequency applied to the targets fixed at 80 V and 200 KHz, respectively. It was found that at lower target current and higher acetylene flow rate a complete poisoning of the Ti targets by the carbonous species (formed by decomposition of acetylene gas) occurred. This obstructed the sputtering of Ti from the targets. Since no Ti was detected by EPMA, these films are pure a-C:H films instead of TiC/a-C:H nanocomposite films (c.f. Table 1). This gave an opportunity to compare the properties of pure a-C:H (single phase) and TiC/a-C:H (two phases) nanocomposite films deposited by 200 kHz p-DC sputtering.

Films were deposited by varying the Ti-target current from 0.6 to 1 A while keeping the substrate bias voltage and C_2H_2 flow rate constant at 80 V and 8 sccm, respectively. Fig. 6a and b shows the frictional characteristics, average CoF and hardness of the films as a function of the current applied to the Ti target. The CoF decreases from 0.15 to 0.05 with increasing Ti-target current from 0.6 to 0.75 A and then increases to 0.09 at 1 A, as seen in Fig 6b. The film deposited at 0.6 A was pure a-C:H and the Ti content in the TiC/a-C:H films deposited at 0.75 and 1 A was approximately 12.5 and 17.5 at.%, respectively. This indicates that for the given range of the Ti content, the TiC/a-C:H nanocomposite films exhibit lower CoF than the pure a-C:H films for the same load and environment conditions. This was mainly due to reduction in the stress in the film with addition of Ti and

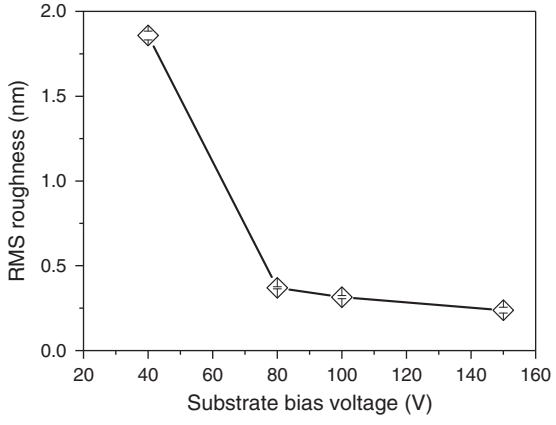

Fig. 5. Surface roughness of 200 kHz p-DC sputtered TiC/a-C:H films as a function of the negative substrate bias voltage.

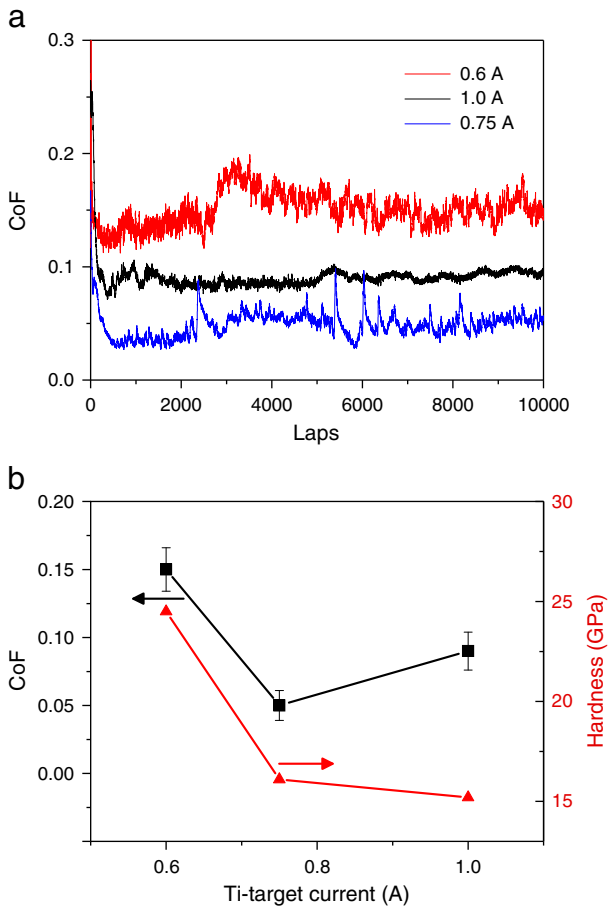

Fig. 6. (a) Friction characteristics of 200 kHz p-DC sputtered a-C:H (deposited at 0.6 A) and TiC/a-C:H films (deposited at 0.75 and 1 A), sliding against steel ball at 5 N normal load, sliding velocity 10 cm/s and a relative humidity of 50% at 23 °C; (b) Plot of CoF (■) and hardness (▲) versus current applied to the Ti target for these films.

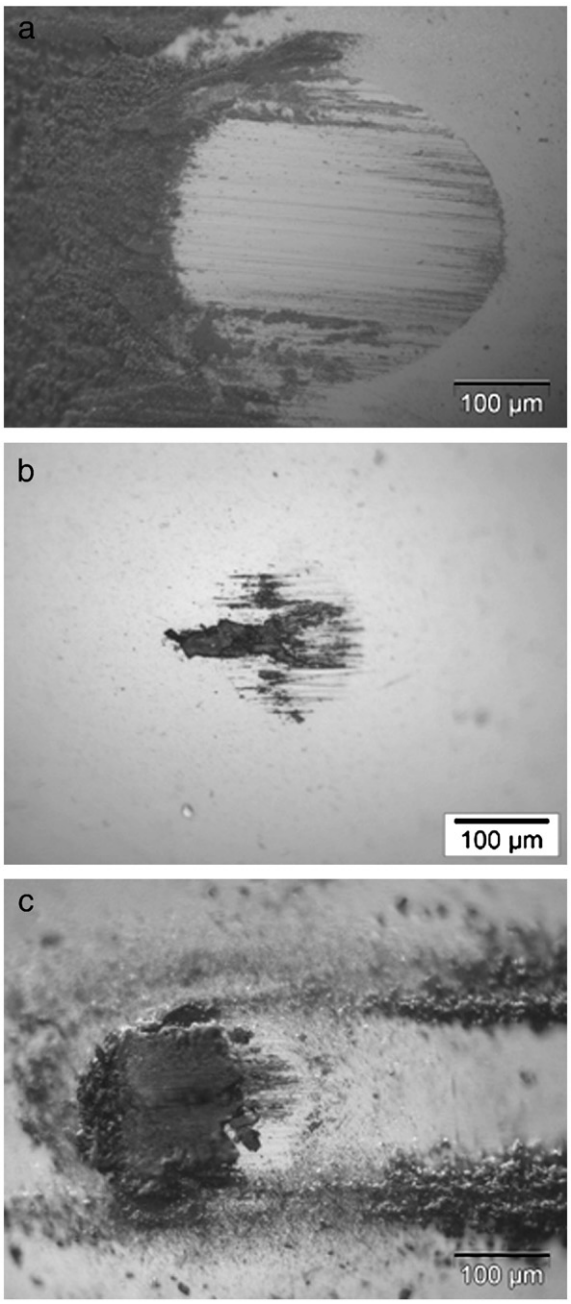

Fig. 7. Optical micrographs of the wear scar on steel balls sliding against the films deposited by 200 kHz p-DC sputtering at a Ti-target current of (a) 0.6 A; (b) 0.75 A and (c) 1 A, respectively. Sliding direction, of the films in contact, from left to right. (The area of transfer layer is larger in (c) than in (b).)

toughening of the film due to TiC nanocrystallites [20] which reduces its brittleness and hence the wear debris formation. Considerable wear debris were found on and around the wear track of the pure a-C:H film due to excessive stress in the film. These hard wear debris cause abrasive wear of the steel ball, which results in a large wear scar of 362 μm in diameter as shown in Fig. 7a. Recently, we have shown that if the contact area on the ball counterpart is large then the transfer layer cannot cover the entire contact area and fails to isolate the steel ball completely and leads to higher CoF [26,31]. Furthermore, the wear debris hinders the formation of a transfer layer [26]. Thus, the transfer layer failed to cover the large contact area on the steel ball and yields higher CoF. A relatively little wear of the steel ball occurred against the TiC/a-C:H nanocomposite films deposited at a Ti-target current of 0.75 and 1 A. As seen in Fig. 7b and c, the wear scar diameters on the steel balls were 145 and 175 μm, respectively. The transfer layer effectively covered the contact area on the steel balls leading to a lower CoF. The TiC nanocrystallites present at the sliding surface enhance the surface graphitization [20] and promote the formation of the transfer layer. Since the concentration of the amorphous lubricant phase determines the frictional behavior, with increasing Ti content from 12.1 to 17.5 at.%, the friction increases from 0.05 to 0.08. A 12 at.% content of Ti was considered as the optimum that gives the lowest CoF of 0.05. Many small yet asymmetric peaks were observed in the plot of CoF versus laps for the film deposited at 0.75 A target current. It was associated with sudden rupture followed by gradual re-formation of the transfer layer during sliding. Once the transfer layer forms on the steel ball, the CoF cannot decrease further and therefore starts to fluctuate. It can be inferred that since the transfer layer covered the sliding surface of the ball, the wear rate of the film diminished. As a result, during further sliding the transfer layer is assumed to get thinner until it breaks down, leading to a sudden rise of the CoF. Sliding at a higher CoF leads to wear of the film which generates the necessary material for the growth of a new transfer layer. Thereafter, a new cycle of the dynamic friction process is repeated. A similar frictional behavior of TiC/a-C:H nanocomposite films was observed in the previous work in our group [20]. This behavior is not seen in the other TiC/a-C:H film, since a partial break down of the transfer layer has a little influence when its area is larger (see Fig. 7c). The hardness of these TiC/a-C:H films was decreased with increasing the Ti-target current. This was mainly attributed to decrease in the sp^3 content in the films as evidenced by the increase in

the I(D)/I(G) ratio and shift of the G peak position to higher wave number (see Table 1) with increasing Ti-target current.

The effect of changing the C_2H_2 flow rates from 8 to 12 sccm, by keeping all other parameters (Ti-target current at 0.75 A and substrate bias at 80 V) constant, on the tribological properties of 200 kHz p-DC sputtered films was also investigated. The EPMA analysis indicated that the film deposited at a flow rate of 8 sccm has 12.1 at.% of Ti whereas the films deposited at a flow rate of 10 and 12 sccm were pure a-C:H films due to complete poisoning of the race tracks on the Ti targets, as explained earlier. The surface roughness of the film increases with increasing C_2H_2 flow rate (See Table 1). Fig. 8a shows the frictional characteristics of these films. It must be noted that this TiC/a-C:H nanocomposite film deposited at 8 sccm flow rate was the same film that gives CoF of 0.05 as discussed in section 3.1. Figs. 7b and 9 show the optical micrographs of the steel balls after sliding against the TiC/a-C:H nanocomposite film and the pure a-C:H films, respectively. A considerable abrasive wear while sliding against the pure a-C:H films increases the contact area on the steel ball, which obstructs effective isolation of the steel ball by the transfer layer and hence lead to higher CoF as explained before. These observations are consistent with the observations in the previous section where the TiC/a-C:H nanocomposite gives lower CoF than the pure a-C:H films and can be explained likewise. In the case of the pure a-C:H films, a higher CoF was observed at 12 sccm than that compared to 10 sccm. The wear scar diameter in the former case was ~558 μm whereas it

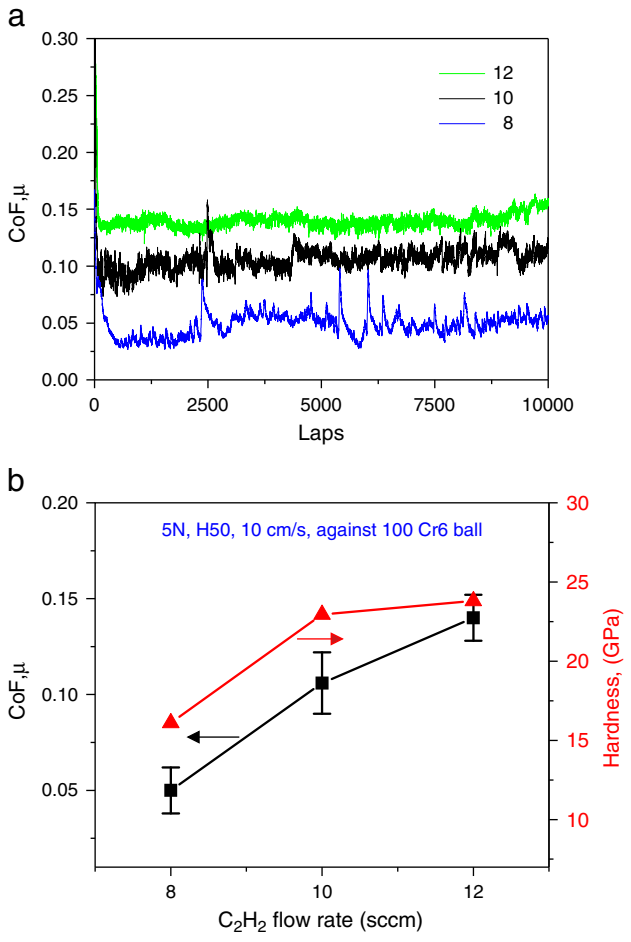

Fig. 8. (a) Friction characteristics of 200 kHz p-DC sputtered films deposited at various flow rates of C2H2 in sccm, as indicated, sliding against steel ball at 5 N normal load, sliding velocity 10 cm/s and a relative humidity of 50% at 23 °C; (b) CoF (■) and hardness (▲) of these films as a function of the C2H2 flow rate. Note that the film deposited at 8 sccm was TiC/a-C:H nanocomposite whereas films deposited at 10 and 12 sccm were pure a-C:H films.

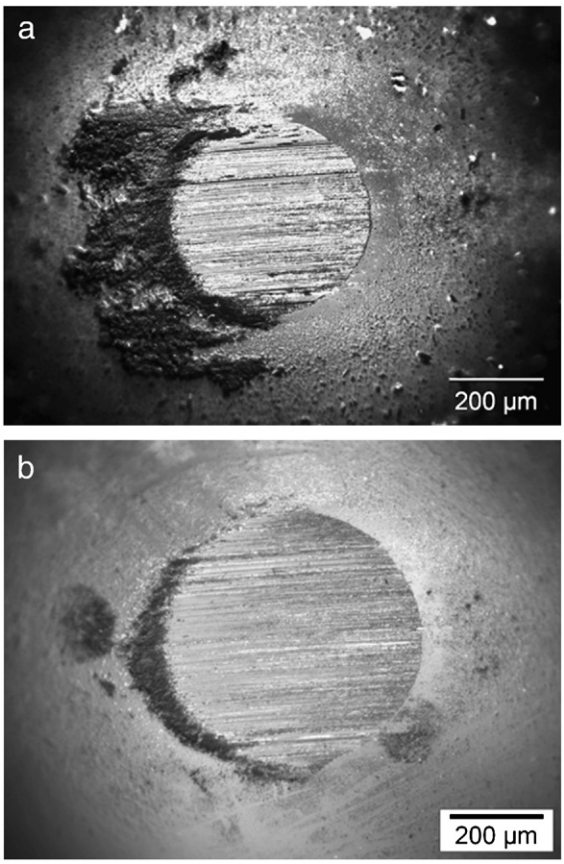

Fig. 9. Optical micrographs of the wear scar on steel balls after sliding against the pure a-C:H films deposited by 200 kHz p-DC sputtering at a C2H2 flow rate of (a) 10 and (b) 12 sccm, respectively. Sliding direction, of the films in contact, from left to right.

was ~427 μm in the latter case. The relatively larger contact area on the steel ball was increasingly difficult to be covered by the transfer layer in the case of the film deposited at 12 sccm and hence leads to higher CoF. A large amount of wear debris were observed on and around the wear track on both these films after the tribotest. The wear debris also contributes to higher CoF as discussed earlier.

Fig. 8b shows the CoF and hardness dependence of these films as a function of the C_2H_2 flow rate. The CoF increases from 0.05 at 8 sccm to 0.14 at 12 sccm. The hardness shows increase from 16 GPa deposited at 8 sccm (TiC/a-C:H film) to approximately 23 GPa and remains almost the same at 10 and 12 sccm (pure a-C:H films). Fig. 10 a–c shows the Raman spectra of these films. There was very little difference between the Raman spectra acquired from the films deposited at 10 and 12 sccm. The TiC/a-C:H nanocomposite film, in Fig. 10a, shows a pronounced D peak compared to the pure a-C:H films, as seen in Fig. 10b and c. These observations indicate that incorporation of Ti into the a-C:H matrix increases the sp^2 content in the films. Fig. 10d shows the variation of the I(D)/I(G) ratio and G peak position as a function of the C_2H_2 flow rate. The I(D)/I(G) ratio decreases and the G peak shifts to a lower wavenumber at a higher C_2H_2 flow rate. Both parameters indicate a progressive amorphisation of the sixfold sp^2-bonded rings and increased presence of sp^3 sites in the films. The higher hardness of these films can be correlated to a higher sp^3 content in the film. The wear rates of the TiC/a-C:H nanocomposite film and pure a-C:H film deposited at 12 sccm were 6.6×10^{-8} and 1.07×10^{-7} $mm^3/N\,m$, respectively. The harder (hardness = 23 GPa) a-C:H films exhibit poor wear resistance compared to the softer (hardness = 16 GPa) TiC/a-C:H nanocomposite films. In order to understand this phenomenon, the compressive stress in these films was measured. Fig. 11 shows that the compressive stress in these films increases with the increase in the C_2H_2 flow rate. The

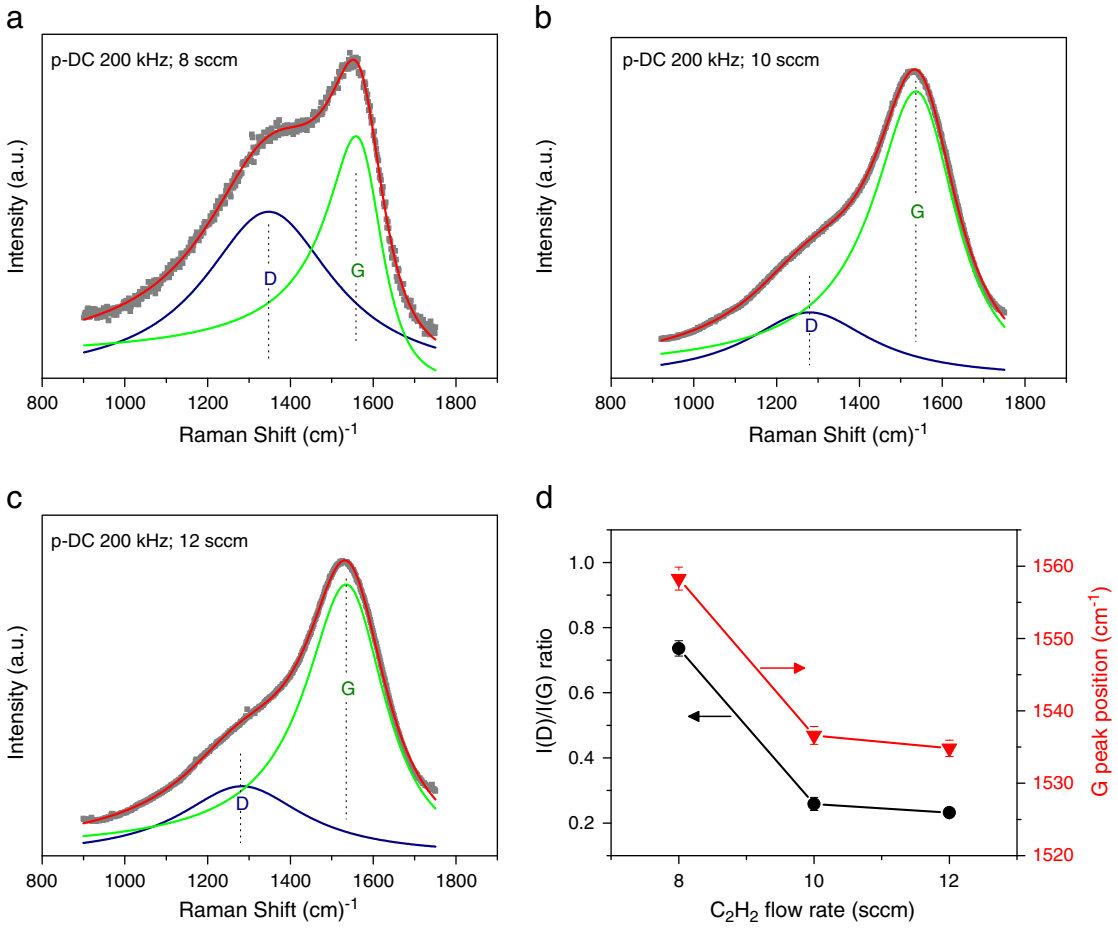

Fig. 10. BWF-Lorentzian fitted Raman spectra of 200 kHz p-DC sputtered films deposited at a C2H2 flow rate of (a) 8 sccm; (b) 10 sccm and (c) 12 sccm; and (d) I(D)/I(G) ratio (●) and G peak position (▼) as a function of the C2H2 flow rate for these films.

compressive stress in the TiC/a-C:H nanocomposite film was less compared to that of pure a-C:H films. This was mainly associated with the higher sp^2 content in the TiC/a-C:H nanocomposite films since only a small increase in the sp^2 content is needed to account for stress release in these films [32]. The increase in the stress in the pure a-C:H films with increasing C_2H_2 flow rate is most likely due to the increase in thickness [33] from ~1.2 μm at 8 sccm to ~1.37 μm at 12 sccm. During sliding, the formation of wear debris was promoted due to the presence of high stress in the film. This also reflects in the high wear rates observed for the a-C:H films (see Table 1). The hard wear debris are detrimental to the tribological properties of these films as discussed earlier.

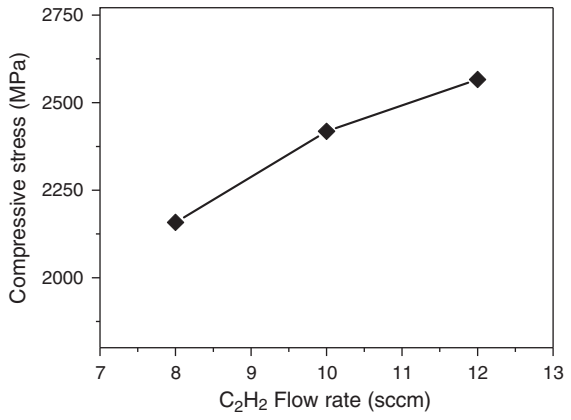

Fig. 11. Compressive stress as a function of the C2H2 flow rate for 200 kHz p-DC sputtered films. The film deposited at 8 sccm was the TiC/a-C:H nanocomposite whereas films deposited at 10 and 12 sccm were pure a-C:H films.

3.4. Effect of pulse frequency

In this section, the effect of pulse frequency (200 and 350 kHz) applied to the Ti targets on the mechanical, structural and tribological properties of the TiC/a-C:H nanocomposite films is discussed. The 200 kHz p-DC sputtered TiC/a-C:H nanocomposite film deposited at 0.75 A Ti-target current, 80 V substrate bias and 8 sccm of C_2H_2 flow rate was considered optimum since it yielded an ultra-low CoF of 0.05 and a low wear rate of 6.6×10^{-8} mm^3/N m. To understand the effect of pulse frequency, a TiC/a-C:H nanocomposite film was deposited by p-DC sputtering at 350 kHz pulse frequency and by keeping all the other parameters unchanged. The properties of these two p-DC sputtered films at 200 and 350 kHz were compared. The cross sectional SEM micrographs shown in Fig. 12 reveal that both these films exhibit a dense and column-free microstructure. The EPMA analysis measured a Ti content of 12.5 and 12.2 at.% in the films deposited at 200 and 350 kHz, respectively. Although the sputtering of the Ti target is less at 350 kHz than at 200 kHz, the chemical composition of these films was comparable within the error limits of the measurements. The energy and flux of Ar^+ ions were much higher at 350 kHz than at 200 kHz p-DC sputtering. The intensive Ar^+ ion impingement at the growing film causes considerable re-sputtering of ad-atoms during deposition. The C atoms were preferentially re-sputtered since they are lighter than the incident Ar ions, whereas Ti atoms being heavier were less likely re-sputtered. During deposition

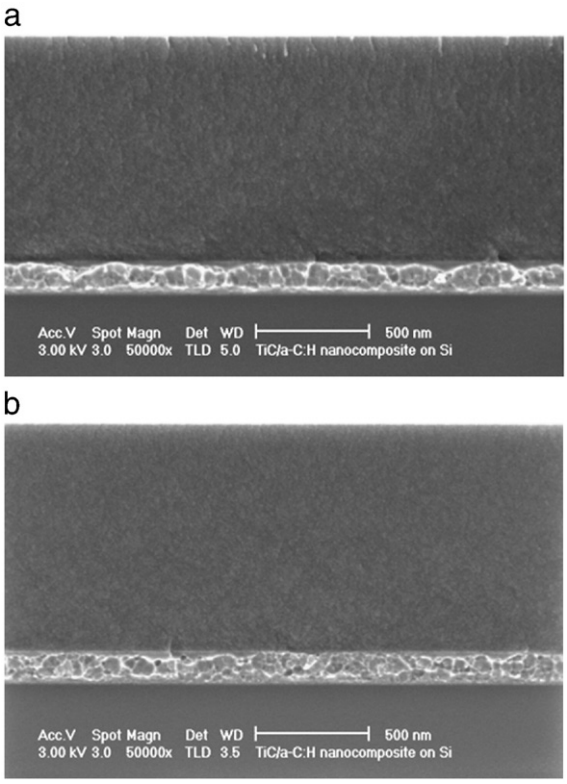

Fig. 12. Cross sectional SEM of TiC/a-C:H nanocomposite films deposited by p-DC sputtering at (a) 200 kHz and (b) 350 kHz pulse frequency.

of the 350 kHz p-DC sputtered film, the sputtering from Ti targets was relatively lower but the re-sputtering of C atom was relatively higher and hence a similar Ti content as that observed for 200 p-DC sputtered film was observed. Fig. 13 shows the grazing incidence XRD spectra for these films confirming the presence of TiC nanocrystallites in these films. The average size of the TiC nanocrystallites was 1.9 and 1.8 nm for the films deposited at 200 and 350 kHz respectively. Several peaks from the Si substrates (dashed lines) were observed in the case of the film deposited at 200 kHz. Moreover these peaks from the Si substrates were shifted to higher 2θ values due to stress in the film and is consistent with the observations made by Zhang et al. [34] during deposition of DLC on Si.

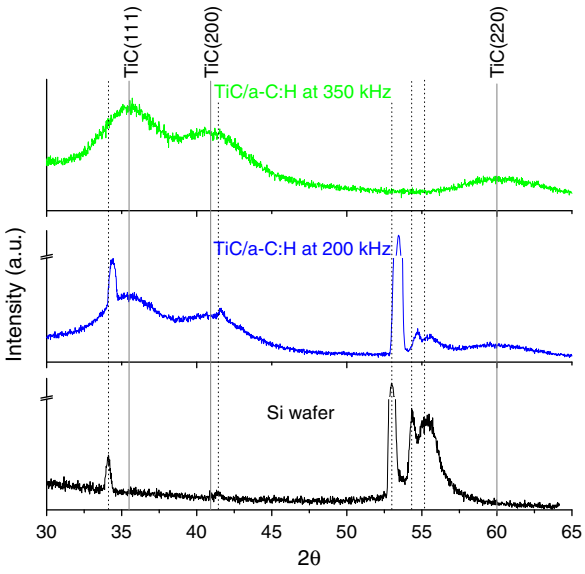

Fig. 13. Grazing incidence XRD spectra for the Si substrate and the TiC/a-C:H nanocomposite films deposited at the indicated pulse frequency. Dashed lines indicate the peaks from the Si substrate.

Fig. 14a shows the Raman spectra acquired from the 350 kHz p-DC sputtered TiC/a-C:H nanocomposite film. This spectra was compared with that of the 200 kHz p-DC sputtered TiC/a-C:H nanocomposite film which is the same as shown in Fig. 10a. The I(D)/I(G) ratio decreases from 0.74 to 0.49 and the G peak shifts from 1558.2 to a lower wave number of 1552.0 with increasing pulse frequency from

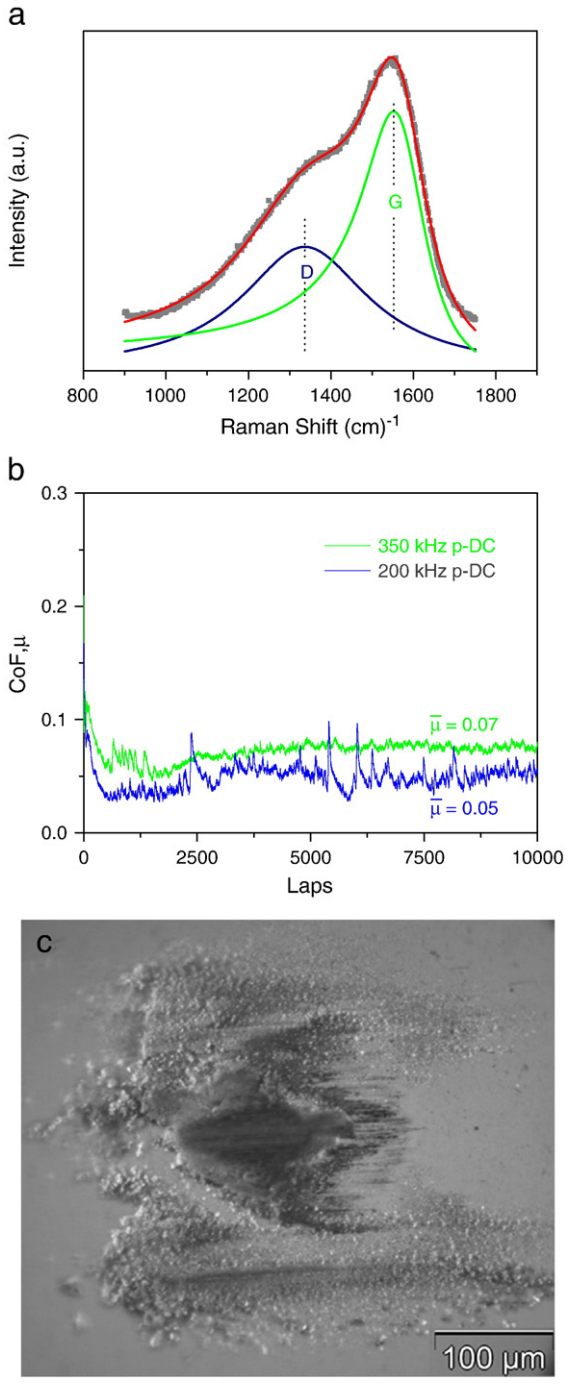

Fig. 14. (a) Raman spectra; and (b) frictional characteristics of the 350 kHz p-DC sputtered TiC/a-C:H nanocomposite film sliding against steel ball (friction graph of 200 kHz p-DC sputtered TiC/a-C:H film in blue color from Fig 6a was included for comparison); (c) optical micrograph of the steel ball after the tribotest. (For interpretation of the references to color in this figure legend, the reader is referred to the web version of this article.)

200 to 350 kHz. Both these observations indicate that the sp^3 content in the 350 kHz p-DC sputtered film is relatively higher than the film deposited at 200 kHz. The mechanism of the formation of sp^3-C is modeled as "subplantation", where energetic C ions are able to penetrate the surface layer and subsequently bond in a highly stressed tetrahedral (sp^3) configuration [35]. For penetration to occur, the ions should overcome the C displacement energy (25–35 eV) [35]. When the majority of C atoms are not ionized, as is the present case of p-DC magnetron sputtering, it can be inferred that more intensive Ar^+ ion impingement to the growing film would promote the formation of sp^3-C. During the deposition, some of the individual C atoms in the surface layer would be knocked-down as a consequence of the energy transfer between the incident Ar^+ ions and C atoms. Since the flux and energy of Ar^+ ions in the case of 350 kHz p-DC sputtering is much higher than that at 200 kHz [15], a higher sp^3 content can be expected. The hardness of the TiC/a-C:H nanocomposite film deposited at 350 kHz was 17.2 GPa which was higher than that observed for the film deposited at 200 kHz (16.1 GPa). It was mainly due to a higher sp^3 content in the 350 kHz p-DC sputtered film. The compressive stress in the films was 2.15 and 2.85 GPa at 200 and 350 kHz pulse frequency, respectively.

Fig. 14b shows the frictional behavior of both the films deposited at 200 and 350 kHz. A higher mean CoF of 0.07 was observed for 350 kHz p-DC sputtered film than that of 0.05 for 200 kHz sputtered film. Figs. 14c and 7b shows the optical micrographs of the wear scar on the steel balls after sliding against 350 and 200 kHz p-DC sputtered TiC/a-C:H films, respectively. In both cases, a transfer layer was formed on the steel ball. The higher CoF can be attributed to the relatively lower amount of the sp^2 content in the film. Moreover, considerable wear debris were formed on and around the wear track on this film and also was collected by the steel ball as seen in Fig. 14c. Due to high hardness of this film, comparatively harder wear debris were formed. The hard wear debris retard the formation of the transfer layer and contribute to high friction. The higher stress in the film deposited at 350 kHz promotes the formation of wear debris during sliding. It also reflects in the higher wear rate of 8.2×10^{-8} $mm^3/(N\,m)$ observed for this film compared to that of 6.6×10^{-8} $mm^3/(N\,m)$ observed for 200 kHz p-DC sputtered TiC/a-C:H film.

It is noted that despite exhibiting higher residual stress compared to that of the pure a-C:H films, the 350 kHz p-DC sputtered TiC/a-C:H nanocomposite film shows lower CoF and better wear resistance (see Table 1). This clearly indicates that incorporation of TiC nanocrystallites into the a-C:H matrix toughens (reduces its brittleness) the film which reduces the wear debris formation during sliding and yields lower friction by promoting surface graphitization.

4. Conclusion

It is shown that dense, tough, ultra-smooth TiC/a-C:H films exhibiting ultra-low friction and excellent wear resistance can be obtained by pulsed-DC sputtering at higher frequencies and at low substrate bias voltage. The important findings in this study comprise:

- Dense, column-free and smooth TiC/a-C:H films can be obtained at a substrate bias voltage of 40 V by p-DC sputtering at 200 and 350 kHz frequency. The tribological properties of TiC/a-C:H nanocomposite films were moderately affected by the change in the substrate bias voltage.
- The change in the phase composition strongly influences the tribological performance where the TiC/a-C:H films perform better than the pure a-C:H films. In the case of TiC/a-C:H nanocomposite films, a higher sp^2 content and the presence of TiC nanocrystallites at the sliding surface promotes formation of the transfer layer and yields lower CoF. The Ti content in the film also influences the tribological performance. The optimal Ti content was determined to be ~12 at.%. In the case of a-C:H films, a relatively higher sp^3 content and residual stress promote the formation of hard wear debris during sliding, which cause abrasive wear and increases the contact area on the ball counterpart. This makes the formation of the transfer layer relatively difficult and leads to higher CoF.
- With increasing pulse frequency, the sp^3 content, hardness and the residual stress in the TiC/a-C:H nanocomposite films increase due to increased intensity of ion impingement to the film. The relatively lower sp^2 content and higher stress in the film deposited at 350 kHz pulse frequency yields inferior tribological properties compared to that observed for TiC/a-C:H film deposited at 200 kHz.

Acknowledgements

This research was carried out under the Project No. MC7.06246 in the framework of the Research Programme of the Materials Innovation Institute M2i (www.M2i.nl), The Netherlands. The authors acknowledge financial support from the M2i. Dr. Paul Bronsveld in the Department of Applied Physics, University of Groningen, The Netherlands is thanked for valuable discussions regarding XRD analysis.

References

[1] S. Veprek, S. Reiprich, Thin Solid Films 268 (1995) 64.
[2] J. Musil, Surf. Coat. Technol. 125 (2000) 322.
[3] A.A. Voevodin, J.S. Zabinski, Diamond Relat. Mater. 7 (1998) 463.
[4] A.A. Voevodin, J.P. O'Neill, J.S. Zabinsky, Surf. Coat. Technol. 119 (1999) 36.
[5] J. Robertson, Mat. Sci. Eng. R37 (2002) 129.
[6] D. Galvan, Y.T. Pei, J.Th.M. De Hosson, Surf. Coat. Technol. 201 (2006) 590.
[7] A.A. Voevodin, J.S. Zabinski, J. Mater. Sci. 33 (1998) 319.
[8] W.J. Meng, R.C. Tittsworth, L.E. Rehn, Thin Solid Films 222 (2000) 377.
[9] C.Q. Chen, Y.T. Pei, K.P. Shaha, J.Th.M. De Hosson, J. Appl. Phys. 105 (2009) 114314.
[10] J.C. Sánchez-Lopez, D. Martinez-Martinez, C. Lopez-Cartes, A. Fernandez, Surf. Coat. Technol. 202 (2008) 4011.
[11] H. Liepack, K. Bartsch, B. Arnold, H.-D. Bauer, X. Liu, M. Knupfer, A. Leonhardt, Diamond Relat. Mater. 13 (2004) 106.
[12] U. Jansson, E. Lewin, M. Rasander, O. Eriksson, B. Andre, U. Wiklund, Surf. Coat. Technol. (2010), doi:10.1016/j.surfcoat.2010.06.017.
[13] B. Yang, Z.H. Huang, H.T. Gao, X.J. Fan, D.J. Fu, Surf. Coat. Technol. 201 (2007) 6808.
[14] Y. Wang, X. Zhang, X. Wu, H. Zhang, X. Zhang, Appl. Surf. Sci. 254 (2008) 5085.
[15] Y.T. Pei, C.Q. Chen, K.P. Shaha, J.Th.M. De Hosson, J.W. Bradley, S.A. Voronin, M. Cada, Acta Mater. 56 (2008) 696.
[16] P.J. Kelly, C.F. Beevers, P.S. Henderson, R.D. Arnell, J.W. Bradley, H. Backer, Surf. Coat. Technol. 174–175 (2003) 795.
[17] C. Muratore, J.J. Moore, J.A. Rees, Surf. Coat. Technol. 163–164 (2003) 12.
[18] J.W. Bradley, H. Backer, P.J. Kelly, R.D. Arnell, Surf. Coat. Technol. 135 (2001) 221.
[19] A.C. Ferrari, J. Robertson, Phys. Rev. B. 61 (2000) 14095.
[20] Y.T. Pei, D. Galvan, J.Th.M. De Hosson, Acta Mater. 53 (2005) 4505.
[21] Y.T. Pei, K.P. Shaha, C.Q. Chen, R. van der Hulst, A.A. Turkin, D.I. Vainshtein, J.Th.M. De Hosson, Acta Mater. 57 (2009) 5156.
[22] K.P. Shaha, Y.T. Pei, C.Q. Chen, A.A. Turkin, D.I. Vainshtein, J.Th.M. De Hosson, Appl. Phys. Lett. 95 (2009) 223102.
[23] P.J. Kelly, A.A. Onifade, Y. Zhou, G.C.B. Clarke, M. Audronis, J.W. Bradley, Plasma Processes Polym. 4 (2007) 246.
[24] A.A. Voevodin, A.W. Phelps, J.S. Zabinski, M.S. Donley, Diamond Relat. Mater. 5 (1996) 1264.
[25] A. Erdemir, C. Bindal, G.R. Fenske, C. Zuiker, P. Wilbur, Surf. Coat. Technol. 86 (1996) 692.
[26] K.P. Shaha, Y.T. Pei, D. Martinez-Martinez, and J.Th.M. De Hosson, Tribol. Lett. (in press), doi:10.1007/s11249-010-9691-4.
[27] D. Martínez-Martínez, C. Lopez-Cartes, A. Fernandez, J.C. Sanchez-Lopez, Thin Solid Films 517 (2009) 1662.
[28] V. Kulikovsky, P. Bohac, F. Franc, A. Deineka, V. Vorlicek, L. Jastrabik, Diamond Relat. Mater. 10 (2001) 1076.
[29] S. Zhang, H. Xie, X. Zeng, P. Hing, Surf. Coat. Technol. 122 (1999) 219.
[30] M.A. Tamor, W.C. Vassell, K.R. Carduner, Appl. Phys. Lett. 58 (1991) 592.
[31] K.P. Shaha, Y.T. Pei, D. Martinez-Martinez, and J.Th.M. De Hosson, Surf. Coat. Technol. (in press).
[32] A.C. Ferrari, B. Kleinsorge, N.A. Morrison, J. Appl. Phys. 85 (1999) 7191.
[33] D. Sheeja, B.K. Tay, K.W. Leong, C.H. Lee, Diamond Relat. Mater. 11 (2002) 1643.
[34] S. Zhang, H. Xie, X. Zeng, P. Hing, Surf. Coat. Technol. 122 (1999) 219.
[35] Y. Lifshitz, S.R. Kasi, J.W. Rabalais, Phys. Rev. Lett. 62 (1989) 1290.